ELSEVIER

Dyes and Pigments 45 (2000) 209–217

DYES and PIGMENTS

Aggregation of bis(2,4,6-trihydroxyphenyl) squaraine in different solutions

Xiao-Hui Li, Bao-Wen Zhang, Yi Cao *

Laboratory of Photochemistry, Institute of Photograpic Chemistry, The Chinese Academy of Sciences, Beijing 100101, PR China

Received 21 October 1999; received in revised form 24 January 2000; accepted 29 February 2000

Abstract

The theoretical and experimental aggregation behavior of bis(2,4,6-trihydroxyphenyl) squaraine (OHSQ) in ethanol and tetrahydrofuran (THF) is compared. In ethanol, two broad absorption bands at 508 and 540 nm undergo bathochromic shifts to 521 and 580 nm with an increase in concentration. In THF, the single narrow absorption band at 568 nm undergoes a bathochromic shift to 579 nm and a hypsochromic shift to 508 nm when the concentration increases. Quantum calculations suggest that in ethanol the dimer aggregate forms in a face-to-face manner with a separation distance of approximatly 0.4–0.5 nm. In THF, it is suggested that two OHSQ molecules are hydrogen bonded in a head-to-tail manner with angles between them of approximately 100.7 and 143.6°. Similar calculations relate to the trimer in both solvents. Changes of absorption bands with pH explain the H-bonding in aggregates.

Keywords: Aggregation; Squaraine; Quantum calculation

1. Introduction

The aggregation of dyes has been observed as a general phenomenon in the solid state, in LB films and in solutions [1–3]. Squaraine dyes usually have strong and intense absorption bands in the visible and near-infrared regions and possess conductive and semiconductive properties [4]. These characteristics have made them very attractive in a variety of technological applications. Squaraine dyes are widely used as xerographic photoreceptors [5–7], in organic solar cells [8–10] and in optical recording media [11–13]. Their aggregation properties also have been well studied [2,3]. Depending on the orientation of transition dipoles and their spectral characteristics, different types of aggregates are known. Commonly, the J-aggregate, with a ''head-to-tail'', or ''in-line'' transition dipole arrangement, shows a sharp, narrow absorption band, and a red-shift compared to the absorption of the corresponding monomer [14–17]. The H-aggregate, on the other hand, is considered to be arranged in parallel stacks, (''head-to-head'' or ''card pack''), and exhibits a blue-shift of the long wavelength transitions in the absorption spectrum compared to the monomer [18–21]. Blue-shifted or red-shifted transitions, or both, can be observed depending on the orientation of the chromophores and the arrangement of transition dipoles [2]. In some cases, the hydrogen bonds play an especially important role in the aggregation and

* Corresponding author. Fax: +86-10-6487-9375.
E-mail address: g203@ipc.ac.cn (Y. Cao).

0143-7208/00/$ - see front matter
PII: S0143-7208(00)00023-1

are responsible for bathochromic or hypsochromic shifts, or both [22]. Oblique transition dipoles both lower and raise the excited state energy for the composite molecule, and the absorption of the aggregate is thus both bathochromically and hypsochromically shifted.

The absorption spectra of bis(2,4,6-trihydroxyphenyl) squaraine (OHSQ) [23] in dry ethanol and THF solutions seem complex. The aggregation behaviour of OHSQ is investigated both experimentally and by using computational methods in this paper.

2. Experimental

2.1. Materials and methods

OHSQ was synthesized according to a previously published procedure [23], recrystallized twice from glacial acetic acid, and then dried under vacuum. The product was characterized by NMR, MS and IR. Dry ethanol and THF were used as solvents. The solutions of OHSQ for optical measurements were prepared and used at room temperature. The absorption spectra were obtained on a Perkin–Elmer Lambda 20 spectrophotometer; and pH values were measured using a model S-3B pH meter.

2.2. Computational methods

A locally modified version of the MOPAC semiempirical quantum mechanics program [24] performed the computations relating to OHSQ. The AM1 parameter set [25] was used with the standard RTF hamiltonian. Geometry optimization termination criteria were tightened by the keywords "PRECISE" and "GNORM = 0.05".

Conceivable configurations of the OHSQ molecule were energetically screened using the SYBYL molecular mechanics force field and geometry optimizer [26]. Several dimer configurations with low energy molecular mechanics and thus optimized geometries were submitted for AM1 geometry optimization. For each molecule in a dimer aggregate, nature bond orbital analysis [27–29] was performed for the lowest energy optimized ground-state geometry. Starting from the optimized geometry, and rotating the second molecule around the hydrogen bond connecting the two molecules, the geometries of other dimer configurations were obtained. The effect of ethanol was included by adding the ethanol molecule to the structure of OHSQ then rotating them together. The electronic spectra were calculated by HYPERCHEM/CNDO, 10^{-5}/800 ITER.

3. Results and discussion

3.1. Absorption properties of OHSQ

3.1.1. Aggregates of OHSQ in ethanol solution

The absorption spectra of different concentrations of OHSQ in dry ethanol are shown in Fig 1. When OHSQ concentration increases from 0.11×10^{-5} to 0.3×10^{-5} mol/l, two broad monomer absorption bands become apparent at 508 and 540 nm. With a further increase in concentration from 0.65×10^{-5} to 1.09×10^{-5} mol/l, the absorption spectra become broader and a new strongly absorbing sharp band appears at 577 nm. This is attributed to the development of aggregation. As the concentration reaches 1.36×10^{-5} mol/l, an aggregate band at 524 nm appears and increases significantly while the monomer band at 508nm decreases in intensity. Meanwhile the band at 577 nm becomes somewhat broader.

These observations suggest that OHSQ tends to form aggregates in dry ethanol as the concentration increases. The absorption bands at 520 and 580 nm shift by 12 and 40 nm, respectively, which

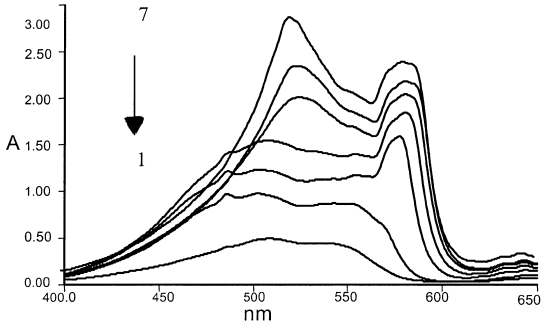

Fig. 1. Absorption spectra of OHSQ in dry ethanol with different concentration of ($\times10^{-5}$ mol/l) (1) 0.11; (2) 0.33; (3) 0.65; (4) 1.09; (5) 1.36; (6) 1.64; (7) 1.91.

implies that the transition dipole of OHSQ in ethanol is arranged in a linear manner [22].

3.1.2. Aggregates of OHSQ in THF solution

The absorption spectra of different concentrations of OHSQ in dry THF are shown in Fig. 2. At concentrations less than 1.6×10^{-5} mol/l, the spectrum consists of a narrow monomer band around 568 nm. At higher concentrations, two new bands round 508 and 579 nm, which are both broader and more intense, predominate. Such a split into two bands, one of which is red-shifted and the other blue-shifted, suggests that the squaraine forms types of aggregates different from those in ethanol.

3.1.3. Relationships between H-bonds of OHSQ aggregates and pH in solution

To further understand the role of H-bonds in the aggregation of OHSQ the pH of OHSQ solutions of 1.09×10^{-5} mol/l in ethanol were changed and the resulting spectra examined. The pH values were increased by addition of KOH [30], and the resulting spectra are shown in Fig. 3.

The many interactions between OHSQ and ethanol in solution make the absorption bands of the spectra in Fig. 3 resistant to simple interpretation. To avoid the solvent effects in ethanol, we investigated the corresponding pH-variant absorption spectra of OHSQ solutions in THF. At low concentrations in THF, OHSQ should form only intramolecular hydrogen bonds, and not OHSQ–solvent intermolecular hydrogen bonds. Changes in pH value should thus influence only this intramolecular hydrogen bond formation. The spectra are shown in Fig. 4. The narrow, high absorption band of OHSQ monomer at pH 4.60 is at about 569 nm. An increase of pH to 5.80 shows a low broad band with a peak at 482 nm. We interpret this change to show the loss of intramolecular H-bonds. The increased basicity of the solution may remove protons from phenyl hydroxyl groups of OHSQ. If all protons are removed, OHSQ will have eight oxide anions, and the resulting great repulsion will cause significant twisting of the OHSQ molecular structure. Any loss of co planarity — any twisting of the system — results in a loss of conjugation, and usually also a shift of absorption maximum to a shorter wavelength [31]. The blue shift observed thus suggests the destruction of intramolecular hydrogen bonds.

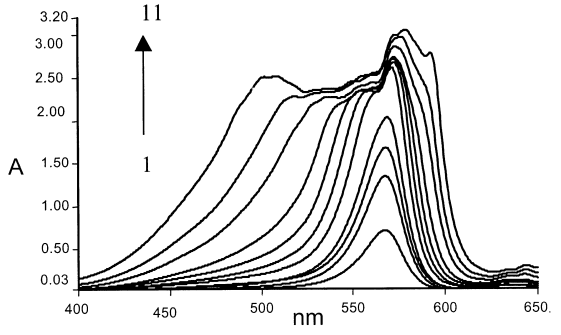

Fig. 2. Absorption spectra of OHSQ in dry THF with different concentration of ($\times10^{-5}$ mol/l) (1) 0.42; (2) 0.76; (3) 1.04; (4) 1.57; (5) 2.08; (6) 2.98; (7) 4.47; (8) 7.45; (9) 16.04; (10) 22.36; (11) 37.27.

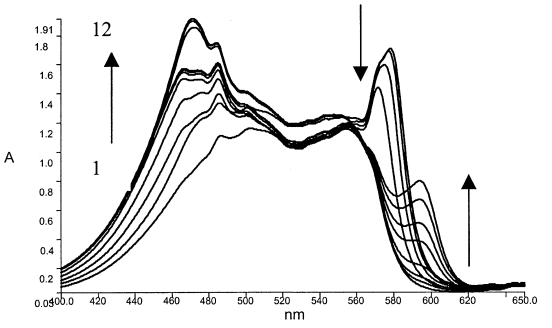

Fig. 3. Absorption spectra of OHSQ in dry ethanol with different pH (1) 5.80; (2) 5.89; (3) 6.00; (4) 6.35; (5) 6.50; (6) 6.83; (7) 7.20; (8) 7.30; (9) 7.38; (10) 7.54; (11) 7.59; (12) 7.80.

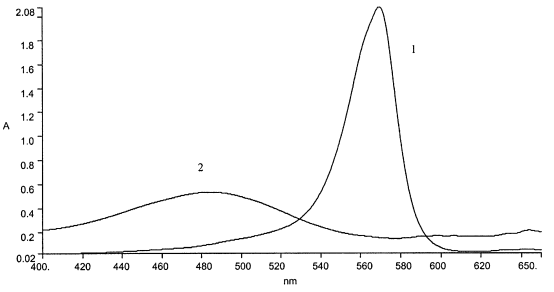

Fig. 4. Absorption spectra of OHSQ in dry THF with different pH (1) 4.61; (2) 5.80.

As observed in Fig. 3, the higher concentration of OHSQ and the H-bond interaction between OHSQ and solvent render the change of absorption behavior with pH more complicated in ethanol than in THF. As initial solution pH of 5.80 increases, the bands near 508 nm blue shift to about 471 nm. This might correspond to a similar oxide anion repulsion suggested above for solutions in THF, or may be due to other types of aggregation. The simultaneous replacement of aggregate bands at about 579 nm with a new band at 594 nm may be considered due to the removal of the hydroxyl group protons on the ends of the aggregate molecules with the addition of KOH.

3.2. Computational chemistry

3.2.1. Calculated data for OHSQ monomer

The ground state energy, dipole moment (DM) and λ_{max} of OHSQ monomer were calculated as described above. The ball-stick structures of OHSQ are showed in Fig. 5a and b. Both the 2-aryl and 4-aryl moieties are twisted with respect to the plane of the cyclobutenone system by twist angles α_2 and α_4, respectively. The minimum energy, together with the maximum absorption wavelength of the two kinds of monomer (with and without intramolecular hydrogen bonds) are given in Table 1.

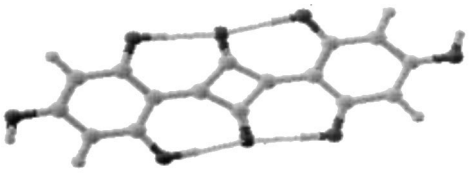

(a)

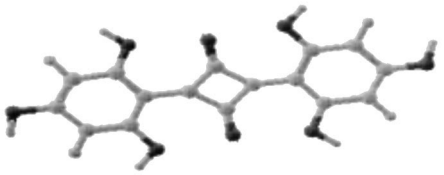

(b)

Fig. 5. (a) Ball-stick structure of OHSQ (having H-bonds). (b) Ball-stick structure of OHSQ.

Table 1
Calculation results of two kinds of monomer OHSQ

	OHSQ (having hydrogen bonds)	OHSQ
E (kcal/mol)	−189.9248	−175.2868
λ (nm)	439.82	489.05
DM	1.09217	0.13035

The computations suggest that the energy of OHSQ with intramolecular hydrogen bonds is lower than that of OHSQ without, since H-bonds always result in a more stable molecular structure. Intramolecular hydrogen bonds exist in both ethanol and THF solution. At the same time, the six hydroxyl groups of an OHSQ molecule can also form a range of intermolecular H-bonds with the hydroxyl groups of ethanol molecules. The two electrons of the oxygen atom in the ground state of a carbonyl group form H-bonds with the solvent. This process decreases the n electron energy level. The reduction of energy approximately equates to the energy of the H-bonds. Since the formation of the intermolecular H-bonds is accompanied by a loss of intramolecular hydrogen bonds, the ground state energy of OHSQ in ethanol seems to be the same as that in THF. However, with an electronic transition to higher energy levels, H-bonds are destroyed. The energy absorbed during the transition includes not only n–π transition, but also enough energy to destroy the H-bonds. Therefore, the total energy should be higher in ethanol than in THF. As found, the λ_{max} of monomer absorption in ethanol should be at shorter wavelength than that in THF.

Table 2
Calculated results of the aggregate in ethanol

r [a] (nm)	H_f (kcal/mol)	DM	λ (nm)	O.S.	$\Delta\lambda$ (nm)[b]
0.35	−361.7243	0.4577	455.28	0.074	15.46
0.40	−369.6407	0.5871	491.77	0.447	51.95
0.45	−371.7451	0.5513	482.83	0.583	43.01
0.50	−372.4532	0.1121	469.01	0.685	29.19
0.55	−372.2263	0.3164	357.19	0.635	−82.63
0.60	−372.363	0.4413	354.89	1.077	−84.93

[a] r is the distance of two OHSQ molecule.
[b] $\Delta\lambda = 439.82 - \lambda$.

Due to the wide range of H-bonds formed in ethanol, it can be concluded a corresponding diversity of molecule configurations exist. The calculated electronic spectrum of OHSQ with hydrogen bonds has a single absorption maximum at approximately 440 nm, while that for OHSQ without hydrogen bonds is at approximate 489 nm.

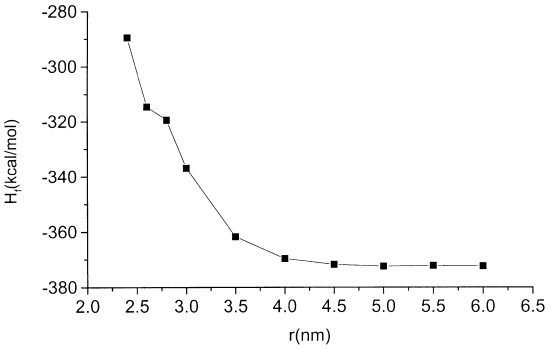

Fig. 6. H_f of the aggregate in ethanol against the distance of two OHSQ molecule.

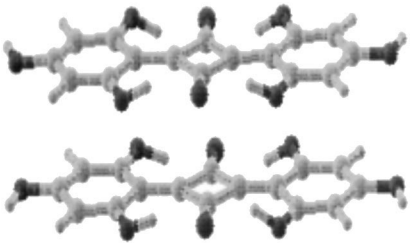

Fig. 7. Aggregate of OHSQ in ethanol.

Table 3
Relationship of H_f and $A_{1\text{-}3\text{-}4}$ in the dimmer molecular of OHSQ in THF solution

$r_{1\text{-}4}$ (nm)	$A_{1\text{-}3\text{-}4}$ (°)	H_f [a] (kcal/mol)	H_f [b] (kcal/mol)	DM [a]	DM [b]
2.9998	163.7	−291.46	−258.5760	1.991	2.5400
2.6999	143.6	−291.84	−258.7661	2.184	3.5658
2.5998	133.1	−250.78	−257.2102	2.242	3.8518
2.4939	124.3	−250.87	−253.8274	2.224	4.2844
2.0999	100.7	−291.92	−259.4911	2.052	3.8115
1.9990	94.8	−291.25	−258.3369	2.239	4.2004
1.8572	87.4	−288.86	−255.854	2.582	4.9256
1.6071	64.9	−286.22	−34.1162	2.079	6.5310

[a] H_f and DM are calculated by molecular mechanics.
[b] H_f and DM are calculated by AM1.

Since each transition from ground state to excited state may result in a spectral absorption band, the breadth of the spectrum of OHSQ in ethanol suggests that there are several different

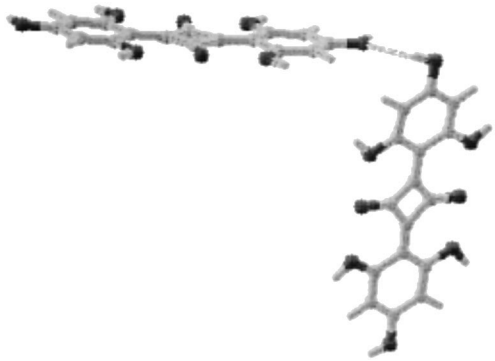

Fig. 8. Aggregate of OHSQ in THF.

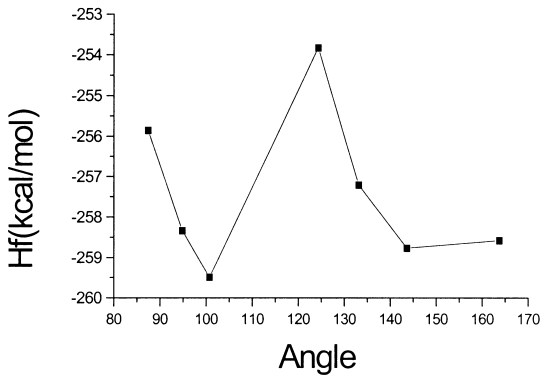

Fig. 9. Relationship of H_f (AM1) and the angle of the two molecules in THF.

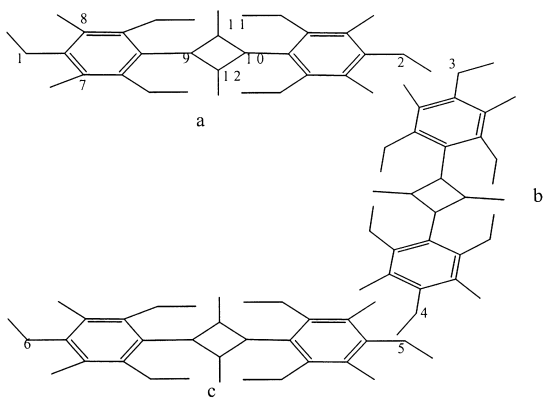

Fig. 10. The serial number in OHSQ trimer.

Table 4
Calculated results of trimer by MOPAC and HYPERCHEM

	In ethanol		In THF
	Trimer I	Trimer I	Trimer III
H_f (kcal/mol)	−544.5318	−564.6084	−465.96
DM	6.9085	4.6779	4.882
λ (nm)	362.78	467.70	445.8
O.S.	0.573	1.160	0.0142

configurations, consisting of OHSQ and from one to eight ethanol molecules. Every one of the six hydroxyl groups in an OHSQ molecule can form a hydrogen bond with ethanol. At the same time four of the phenyl hydroxyl groups can form intra- and/or intermolecular H-bonds with the two oxygen atoms on the cyclobutenone, contributing further to the diversity of molecular configuration in ethanol. The lower polarity of THF and its lack of active

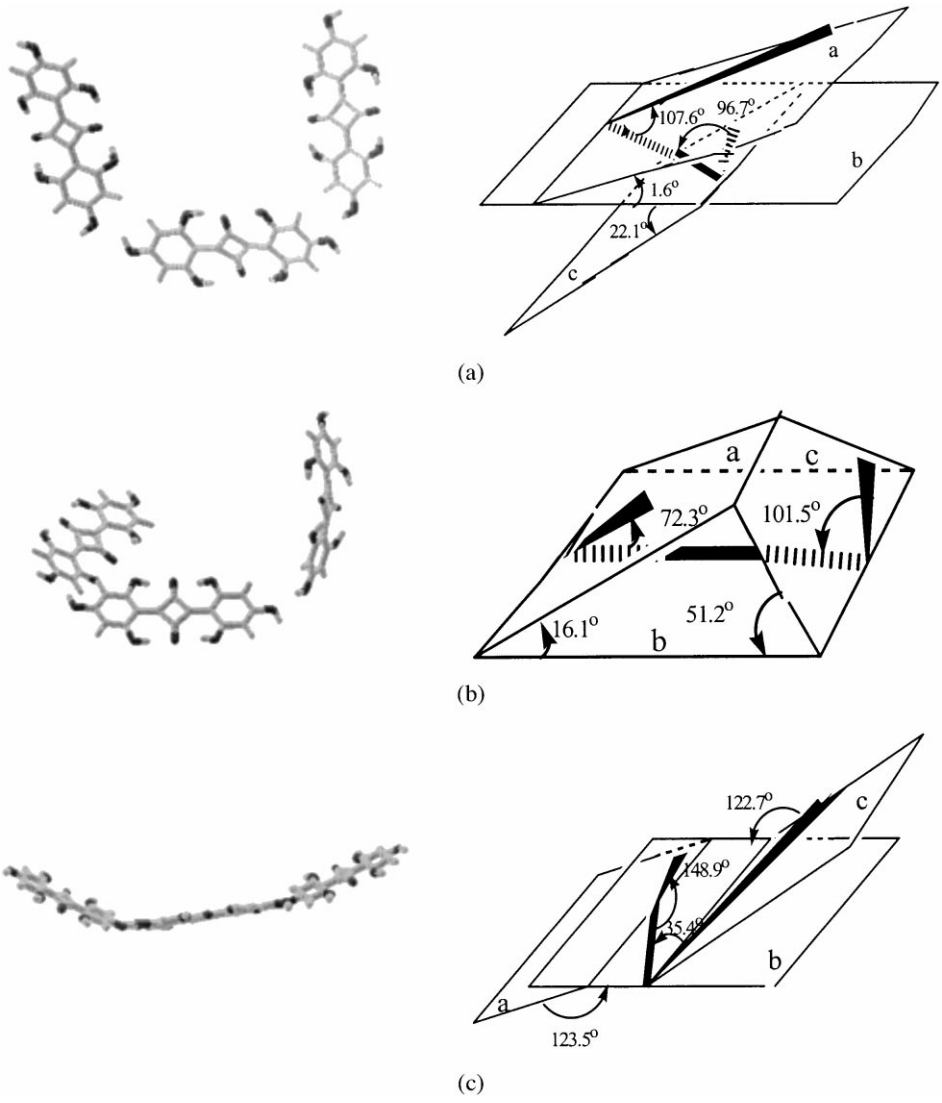

Fig. 11. (a) Trimer aggregate in ethanol (and the Fischer projection structure). (b) Trimer aggregate in ethanol (and the Fischer projection structure). (c) Trimer aggregate in THF (and the Fischer projection structure).

hydrogen atoms give rise to an OHSQ monomer spectrum that is considerably simpler and narrower.

3.2.2. Dimer aggregate

3.2.2.1. Dimer aggregate in ethanol. The involvement of OHSQ hydroxyl groups in OHSQ–solvent intermolecular H-bonds in ethanol prevents the formation of a linear (''head-to-head''or ''tail-to-tail'') form of the OHSQ dimer aggregate. The calculations for solutions in ethanol indicate that the van der Waals force gives the 'face-to-face' OHSQ aggregate with a distance larger than 0.4 nm between the two molecules, the lowest energy and the most steady state. This is shown in Table 2 and Fig. 6. As the distance exceeds 0.5 nm, however, the van der Waals force between the two molecules is too low to form the aggregate: the calculated absorption wavelength is blue shifted and does not match the experimental spectrum. When the distance is from 0.4 to 0.5 nm, the spectrum's calculated red shift is to 492 and 469 nm, respectively. It is concluded, therefore, that the aggregate in ethanol is in the face-to-face form, with an intermolecular distance of between 0.4 and 0.5 nm, as shown in Fig. 7.

3.2.2.2. Dimer aggregate in THF. The H_f and *DM* derived from molecular mechanics and AM1 calculations, and the angle between the two molecules in the aggregate in THF, are summarized in Table 3 and can be seen in Fig. 8 (where the serial numbers of the first two molecules are the same as in Fig. 10).

Since there are only intramolecular OHSQ hydrogen bonds in THF, the two para-hydroxyl groups in OHSQ can easily form H-bonds with the corresponding groups in other OHSQ molecules. The aggregates were thus designed in a ''hand-in-hand'' manner with angles as shown in Fig. 9. The total energy and the *DM* reach a maximum at an angle of 124.3° between the two OHSQ molecules in THF, which suggests that the aggregate with this angle is the least stable, and probably can not exist. The lowest calculated energy is for angles of 100.7 and of 143.6°, and corresponds with the stability of these angles shown in Fig. 9. The broader absorption bands of the aggregate spectrum than that of the monomer means there are several manners of aggregation in THF, possibly a range with angles of around 100.7 and 143.6° between the two molecules.

3.2.3. Trimer aggregate

On the assumption that OHSQ can aggregate in both dimer and trimer forms, a range of three-molecule aggregates were designed and calculated by MOPAC and HYPERCHEM. Of the numerous possibilities, MOPAC and HYPERCHEM generated results for three types of trimer, which are shown in Table 4. These three types of aggregates, which have the lowest calculated H_f values, are listed in Fig. 11a–c, together with their Fischer projection structures. The data for these trimer types of OHSQ is summarized in Table 5, and includes intermolecular angles and intramolecular angles in each. The serial numbers of three OHSQ molecules are shown in Fig. 10.

3.2.3.1. Trimer aggregate in ethanol solution. As shown in Fig. 11a and b, the three molecules of OHSQ trimer are not in one plane but in three. The angles between the molecular axes (on planes a, b and c) are shown in the Fischer projection structures.

The higher H_f and higher O.D. of trimer I make it less stable than trimer II. The calculated λ_{max} of trimer I is 362.78 nm, while that of trimer II is

Table 5
Angles calculated by MOPAC

A (°)	Trimer I	Trimer II	Trimer III
1-2-5	98.7	65.8	146.2
2-5-6	86.2	91.9	143.5
1-5-6	53.3	65.0	136.6
1-3-4 (angle of a and b)	107.6	72.3	148.9
1-2-3-4 (dihedral angle of a and b)	1.6	16.1	−123.5
3-4-5-6 (dihedral angle of b and c)	−22.1	51.2	122.7
3-5-6	96.7	101.5	35.4
6-4-3	180	170.4	0
7-8-11-12	−13.6	55.9	15.8
5-6-1-2 (dihedral angle of c and a)	105.0	71.1	-3.0
4-2-1	94.8	102.2	0
7-8-9-10	156.6	−167.3	177.3

Table 6
Experimental λ (nm) results and calculated results of OHSQ

	λ (monomer)	λ (dimer)	λ (trimer)	$\Delta\lambda$	
				Red-shift	Blue-shift
In ethanol [a]	508	521		13	
	540	580		40	
In ethanol [b]	440	461–490.1	362.78	21–50.1 (dimer)	77.22 (trimer)
			467.70	27.7 (trimer)	77.22 (trimer)
In THF [a]	568	508			60
		579		11	
In THF [b]	440	385.22	445.8	5.8 (trimer)	55.22 (dimer)

[a] Experimental.
[b] Calculated.

467.70 nm. Compared to the calculated λ_{max} of the monomer in ethanol, the λ_{max} of trimer I is blue-shifted by 77.22 nm that of trimer II is red-shifted by 27.70 nm. The unstable energy and the high O.D of trimer I account for the lack of agreement between theory and experiment.

3.2.3.2. Trimer aggregate in THF solution. Trimer III is formed in a "hand-in-hand" manner. As can be seen from Fig. 11c and the Fischer projection structure, the three molecules are in three separate planes (a, b and c).

3.2.4. Contrast of experimental and calculated results

Experimental and calculated λ_{max} results for OHSQ are summarized in Table 6. The experimental λ_{max} values in ethanol for the aggregate are red-shifted by 13 and 40 nm compared to those for the monomer. The calculated λ_{max} values of dimer are red-shifted by 21 and 50.1 nm from the single calculated maximum for the monomer, while for the trimer one of the two maxima is red-shifted 27.7 nm and the other is blue-shifted 77.22 nm. In THF, the experimental λ_{max} values of the aggregate are red-shifted 11 nm and blue-shifted 60 nm from those of the single monomer peak. The calculated λ_{max} of the dimer is blue-shifted by 55.22 nm and the trimer red-shifted by 5.8nm compared to that calculated for the monomer.

4. Conclusions

The properties of OHSQ and its aggregation in dry ethanol and THF solutions have been examined. OHSQ shows two broad absorption bands at 508 and 540 nm in ethanol which red-shift to 521 and 580 nm respectively as the concentration increases. In THF a narrow band at 568 nm splits into a red-shifted peak at 579 nm and a blue-shifted peak at 508 nm when concentration increases.

Conventional J-aggregate and H-aggregate models cannot explain the complex experimental spectra exactly. We have used quantum calculations (specifically MOPAC and HYPERCHEM) to compute theoretical spectra. The results indicate that in ethanol the dimer aggregate favors a "face-to-face" arrangement with an intermolecular distance of approximately 0.4–0.5 nm. The trimer aggregates form with a dihedral angle of 1.6 and 22.1° for trimer I, and 16.1 and 51.2° for trimer II. In THF, two OHSQ molecules form a "head-to-tail" dimer with angles between two molecules of 100.7 or 143.6°. The trimer aggregates form in a "hand-in-hand" manner with dihedral angles of −123.5 and 122.7°.

The changes in absorption bands with change in pH reinforces evidence derived from the quantum calculations, namely that the hydrogen bonds play an important role in the formation of aggregate.

Acknowledgements

This work is supported by NNSFC (59790050, 29971031). The authors would like to thank Professor Yan Dayu for his great help with Computational work.

References

[1] Yuzhakov VI. Russ Chem Rev (Engl Transl) 1979;48:1076.
[2] Chen H, Law KY, Whitten DG. J Phys Chem 1996;100:5949–55.
[3] Buncel E, Mckerrow AJ, Kazmaier P. J Chem Soc, Chem Commun 1992: 1242-3.
[4] Law KY. J Phys Chem 1987;91:5184.
[5] Law KY, Bailey FC. J Imaging Sci 1987;31:172.
[6] Tam AC, Balanson RD. IBM J Res Develop 1982;26:186.
[7] Wingard RE. IEEE Ind Appl 1982; 1251.
[8] Loutfy RO, Hsiao CK, Kazmaier PM. Photogr Sci Eng 1983;27:5.
[9] Morel DL. Mol Cryst Lio Cryst 1979;50:127.
[10] Zhao W, Hou YJ, Wang XS et al. Solar Energy Materials & Solar Cells 1999;58:173–83.
[11] Gravesteijn DJ, Steenbergen C, Vander Veen J. Proc SPIE Int Soc Opt Eng 1988;420:327.
[12] Jipson VP, Jones CR. J Vac Sci Technol 1981;18:105.
[13] Jipson VP, Jones CR. IBM Tech Discl Bull 1981;24:298.
[14] Jelly EE. Nature 1936;138:1009.
[15] Kawaguchi J, Iwata K. Thin Solid Films 1990;191:173.
[16] Vaidyanathan S, Patterson LK, Mobius D, Gruniger HR. J Phys Chem 1985;89:491–7.
[17] Nakahara H, Fukuda K, Mobius D, Kuhn H. J Phys Chem 1986;90:6144–8.
[18] Moony WF, Whitten DG et al. J Am Chem Soc 1984;106:5659.
[19] Heesemen J. J Am Chem Soc 1980;102:2167.
[20] Emerson ES, Conlin MA, Rosenoff AE, Norland KS, Rodriguez H, Chin D, Bird GR. J Phys Chem 1967;71(8):2396–403.
[21] Evans CE, Song Q, Bohn PW. J Phys Chem 1993;97:12302.
[22] Kasha M, Rawls HR, El-Bayoumi MA. Pure Appl Chem 1965;11:371–92.
[23] Tribes A, Jacob K. Angew Chem, Int Ed Engl 1965;4(1):694.
[24] Stewart JJP, MOPAC Version 5.0, Frank J. Seiler Research Laboratory, US Air Force Academy, Colorado Springs, CO 80840. [Available through the Quantum Chemistry Program Exchange (QCPE). The version used in the present work was heavily modified by J. T. Blair.]
[25] Dewar MTS, Zoebisch EG, Healay EF, Stewart JJP. J Am Chem Soc 1985;107:3902–9.
[26] Clark M, Cramer III MD, Openbosch NV. J Comput Chem 1989;10:982.
[27] Carpenter JE, Weinhold F. J Mol Struct (Theochem) 1988;196.
[28] Reed AE, Weinstock RB, Weinhold F. J Chem Phys 1985;83:735.
[29] Reed AE, Weinhold F. J Chem Phys 1983;78:4066.
[30] Griffiths J, Mama J. Dyes and Pigments 2000;44:9–17.
[31] Jurkowith L, Loeb JN, Brown PK, Wold G. Nature, No. 4686, p. 614, 22 August, 1959.